# Chalmers Publication Library

## Fullerene mixtures enhance the thermal stability of a non-crystalline polymer solar cell blend

(article starts on next page)

# Fullerene mixtures enhance the thermal stability of a non-crystalline polymer solar cell blend

Camilla Lindqvist, Jonas Bergqvist, Olof Bäcke, Stefan Gustafsson, Ergang Wang, Eva Olsson, Olle Inganäs, Mats R. Andersson, and Christian Müller

## Articles you may be interested in

Investigation on the effects of thermal annealing on PCDTBT:PCBM bulk-heterojunction polymer solar cells
AIP Conf. Proc. **1512**, 776 (2013); 10.1063/1.4791268

Nanostructured electrodes for organic bulk heterojunction solar cells: Model study using carbon nanotube dispersed polythiophene-fullerene blend devices
J. Appl. Phys. **110**, 064307 (2011); 10.1063/1.3633236

Thermal stability of amorphous silicon/silicon nitride stacks for passivating crystalline silicon solar cells
Appl. Phys. Lett. **93**, 173502 (2008); 10.1063/1.3009571

Observation of the subgap optical absorption in polymer-fullerene blend solar cells
Appl. Phys. Lett. **88**, 052113 (2006); 10.1063/1.2171492

Light intensity dependence of open-circuit voltage of polymer:fullerene solar cells
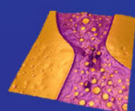Appl. Phys. Lett. **86**, 123509 (2005); 10.1063/1.1889240
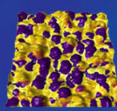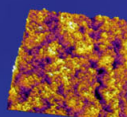
# Fullerene mixtures enhance the thermal stability of a non-crystalline polymer solar cell blend

Camilla Lindqvist,[1] Jonas Bergqvist,[2] Olof Bäcke,[3] Stefan Gustafsson,[3] Ergang Wang,[1] Eva Olsson,[3] Olle Inganäs,[2] Mats R. Andersson,[1,4] and Christian Müller[1,a)]

[1]*Department of Chemical and Biological Engineering/Polymer Technology, Chalmers University of Technology, 41296 Göteborg, Sweden*
[2]*Department of Physics, Chemistry and Biology, Linköping University, 58183 Linköping, Sweden*
[3]*Department of Applied Physics, Chalmers University of Technology, 41296 Göteborg, Sweden*
[4]*Ian Wark Research Institute, University of South Australia, Mawson Lakes, South Australia 5095, Australia*

Printing of polymer:fullerene solar cells at high speed requires annealing at temperatures up to 140 °C. However, bulk-heterojunction blends that comprise a non-crystalline donor polymer often suffer from insufficient thermal stability and hence rapidly coarsen upon annealing above the glass transition temperature of the blend. In addition, micrometer-sized fullerene crystals grow, which are detrimental for the solar cell performance. In this manuscript, we present a strategy to limit fullerene crystallization, which is based on the use of fullerene mixtures of the two most common derivatives, $PC_{61}BM$ and $PC_{71}BM$, as the acceptor material. Blends of this fullerene mixture and a non-crystalline thiophene-quinoxaline copolymer display considerably enhanced thermal stability and largely retain their photovoltaic performance upon annealing at elevated temperatures as high as 170 °C. © 2014 AIP Publishing LLC. [http://dx.doi.org/10.1063/1.4870997]

Polymer solar cells have gained a large research interest during the last decade. A big palette of promising conjugated polymers has been developed, which today offers solar cell efficiencies of up to 9%–10% for lab-scale devices.[1,2] The active layer of polymer solar cells consists of a fine blend of a donor polymer and an electron accepting material, such as a fullerene derivative, and the precise blend nanostructure is critical for achieving a high photovoltaic performance. One advantage of polymer:fullerene solar cells is the possibility to use roll-to-roll printing processes for device production. In order to implement a high-throughput printing process, several heating steps are required to achieve rapid solvent removal. The most likely substrate is polyethylene terephthalate (PET), which permits processing temperatures of up to 140 °C.[3,4] Hence, it is critical that the polymer:fullerene blend nanostructure is thermally stable at these conditions.

After deposition from solution, polymer:fullerene blends tend to adopt a non-equilibrium nanostructure, which can be preserved as long as the material is kept below the blend glass transition temperature ($T_g^{blend}$).[5–8] However, polymer:fullerene blends tend to coarsen when heated above $T_g^{blend}$, which for the majority of currently investigated materials lies below the required processing and operating temperatures. In addition, micrometer-sized fullerene crystallites grow,[9,10] which are detrimental for the device performance.[5,8,11]

One increasingly explored route to improve the thermal stability of polymer:fullerene blends is the use of fullerene mixtures, which either hinders crystallization of the fullerene acceptor,[12–14] or results in the controlled nucleation of sub-micrometer-sized fullerene crystals.[15,16] Here, mixtures of phenyl-$C_{61}$-butyric acid methyl ester ($PC_{61}BM$, Fig. 1) and phenyl-$C_{71}$-butyric acid methyl ester ($PC_{71}BM$, Fig. 1) are particularly attractive since a $C_{60}$:$C_{70}$ mixture with a typical

ratio of about 4:1 is the immediate product that is obtained from fullerene synthesis.[17,18] Hence, PCBM mixtures can be prepared without the need for separation of the $C_{60}$:$C_{70}$ mixture, which is likely to reduce the cost of the acceptor material. Importantly, since $PC_{61}BM$ and $PC_{71}BM$ feature the same lowest unoccupied molecular orbital (LUMO) the use of PCBM mixtures does not negatively influence the efficiency of polymer solar cells.[19,20] In fact, for devices based on a phenylene-quinoxaline or a polyfluorene-benzothiadiazole copolymer and $PC_{61}BM$:$PC_{71}BM$ mixtures an enhanced short-circuit current ($J_{sc}$) has been reported, whereas the fill factor ($FF$) and the open-circuit voltage ($V_{oc}$) remained unaffected compared to devices with neat $PC_{61}BM$.[19]

Recently, we have investigated the thermal stability of blends comprising the copolymer poly[2,3-bis-(3-octyloxyphenyl)-quinoxaline-5,8-diyl-*alt*-thiophene-2,5-diyl] (TQ1, Fig. 1)
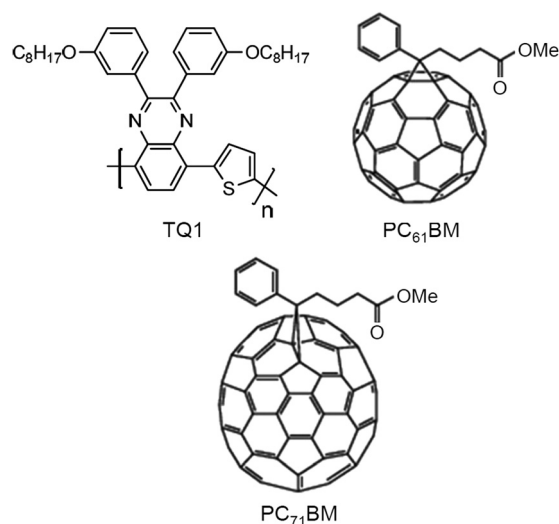


FIG. 1. Chemical structures of TQ1, $PC_{61}BM$, and $PC_{71}BM$.

a)christian.muller@chalmers.se

and $PC_{61}BM$.[8] TQ1 is a non-crystalline donor material that features a high glass transition temperature $T_g^{TQ1} \sim 100\,°C$ (Refs. 21 and 22) and permits solar cell efficiencies of up to 6%–7%.[23,24] We found that the solar cell performance of $TQ1:PC_{61}BM$ rapidly deteriorated when heated above $T_g^{blend} \sim 110\,°C$ due to coarsening of the blend nanostructure as well as the formation of micrometer-sized fullerene crystals. Here, we explore to which extent the thermal stability can be improved by instead using PCBM mixtures as the acceptor material.

In the first set of experiments, we examined the thermal behavior of PCBM mixtures ($PC_{61}BM$ and $PC_{71}BM$ purchased separately from Solenne BV, purity > 99%). First heating thermograms of solution-cast material, recorded with a Perkin Elmer Pyris 1 Differential scanning calorimetry (DSC), reveal that the peak melting temperature of neat $PC_{61}BM$, $T_m^{PC_{61}BM} \sim 280\,°C$, decreased by about $20\,°C$ when only 10 wt. % of $PC_{71}BM$ was added (Figure 2(a)). For mixtures containing 20 wt. % $PC_{71}BM$, in the following referred to as $PCBM_{8:2}$, no melting endotherm was recorded, which suggests that this stoichiometry tends to form amorphous solids.

We used optical microscopy to examine to which extent the thermal behavior of $PC_{61}BM$, $PC_{71}BM$, and their mixtures also persists when blended with TQ1 (number-average
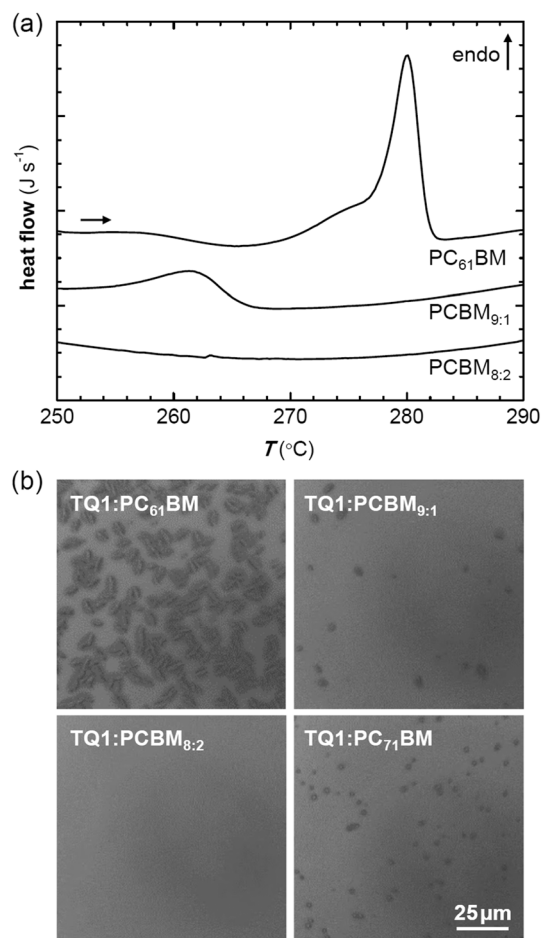
molecular weight $M_n \sim 71\,kg\,mol^{-1}$; polydispersity index- $\sim 3.7$). To this end, 1:1 TQ1:PCBM films with were spin-coated from *ortho*-dichlorobenzene (oDCB, $25\,g\,L^{-1}$) solutions and annealed at $170\,°C$ for 10 min. Optical micrographs of neat $TQ1:PC_{61}BM$ and $TQ1:PC_{71}BM$ films feature distinct, micrometer-sized fullerene crystals (Fig. 2(b)). Furthermore, we find that for $PCBM_{9:1}$ the amount of crystals has decreased significantly and for $PCBM_{8:2}$ no fullerene crystals can be discerned. This is corroborated by UV-vis spectra of annealed films, which show a clear decrease in light transmission below the bandgap of the polymer for $TQ1:PC_{61}BM$ but not $TQ1:PCBM_{8:2}$ after annealing for 10 min at $140\,°C$.[25] We explain the observed invariance in light transmission for samples containing PCBM mixtures with the absence of light scattering from microscopic fullerene crystals.[6,10,26] Evidently, the use of PCBM mixtures that contain 20 wt. % $PC_{71}BM$ strongly hinders fullerene crystallization.

We carried out transmission electron microscopy (TEM) to analyse the nanostructure of $TQ1:PC_{61}BM$ and $TQ1:PCBM_{8:2}$ films in more detail. TEM bright field images and selected area electron diffraction patterns were recorded with a TEM $G^2$ T20 Tecnai instrument at an acceleration voltage of $200\,kV$. TEM images of spin-coated $TQ1:PC_{61}BM$ and $TQ1:PCBM_{8:2}$ films appear homogeneous and no structural changes can be observed for films annealed at $100\,°C$ for 10 min (Fig. 3). Corresponding electron diffraction patterns feature a distinct amorphous halo that indicates disordered fullerene material. However, annealing at $140\,°C$ for 10 min, i.e.,

FIG. 2. (a) DSC first heating thermograms o $PC_{61}BM$, $PCBM_{9:1}$ and $PCBM_{8:2}$. (b) Optical micrographs of 1:1 $TQ1:PC_{61}BM$, $TQ1:PCBM_{9:1}$, $TQ1:PCBM_{8:2}$, and $TQ1:PC_{71}BM$ films after annealing at $170\,°C$.
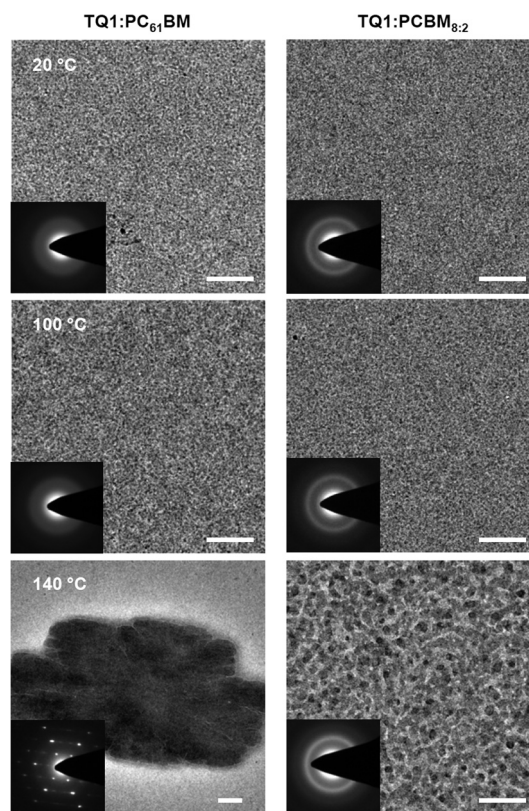
FIG. 3. TEM micrographs of $TQ1:PC_{61}BM$ (left panel) and $TQ1:PCBM_{8:2}$ films (right panel) annealed for 10 min at the indicated temperatures. Insets are corresponding electron diffraction patterns. Scale bar corresponds to 200 nm.
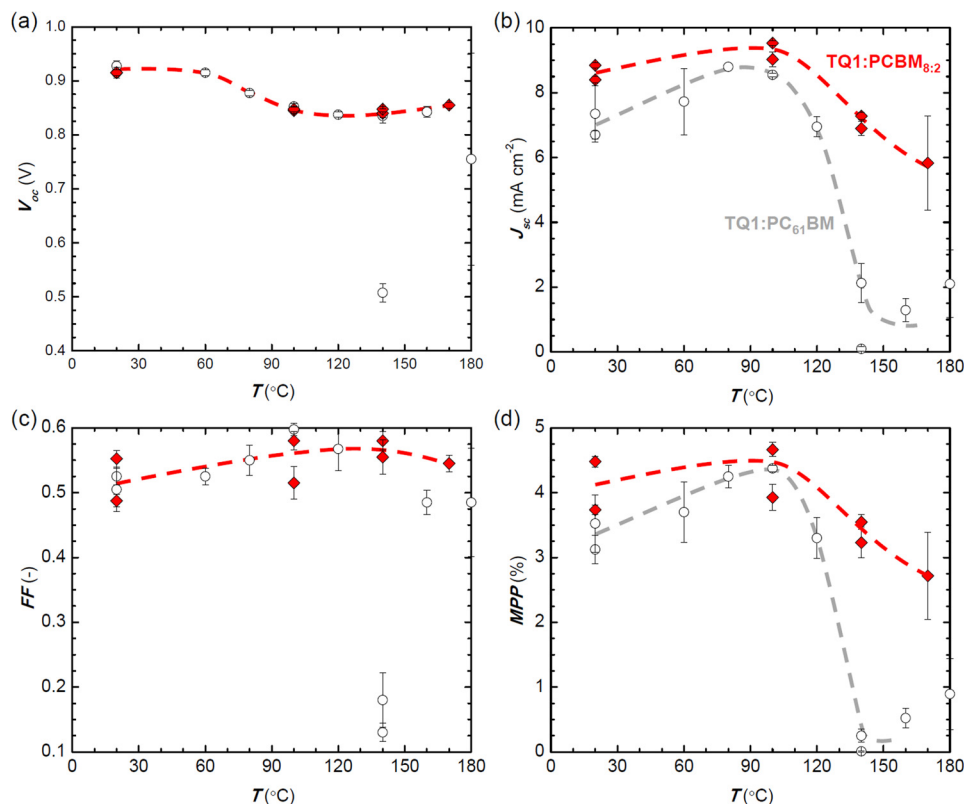
FIG. 4. (a) $V_{oc}$, (b) $J_{sc}$, (c) $FF$, and (d) MPP as a function of active layer annealing temperature for 1:1 TQ1:$PC_{61}BM$ (open circles; data taken from Ref. [8]) and TQ1:$PCBM_{8:2}$ (red diamonds). Error bars indicate the standard deviation of four devices on the same substrate. Dashed lines are a guide to the eye.

above $T_g^{blend} \sim 110\,°C$, results in distinctly different nanostructures. In accordance with our previous report TQ1:$PC_{61}BM$ films feature micrometer-sized $PC_{61}BM$ crystals, as confirmed by single-crystal like electron diffraction patterns that agree with previously published work.[9,10] In contrast, for TQ1:$PCBM_{8:2}$, we observe a coarser nanostructure with $\sim 50$ nanometer-large domains that remain disordered as evidenced by the conspicuous absence of sharp diffraction spots in corresponding electron diffraction patterns.

Finally, we investigated the photovoltaic performance of TQ1:$PCBM_{8:2}$ solar cells before and after annealing of the active layer, which we compare with corresponding TQ1:$PC_{61}BM$ devices that we have studied previously.[8] Devices with an architecture of glass/ITO/PEDOT:PSS/active layer/LiF/Al were prepared by spin-coating active layers from 25 g L$^{-1}$ $o$DCB solution on top of PEDOT:PSS (Clevios P VP Al 4083, Heraeus; annealed at $125\,°C$ for $\sim 15$ min). After spin-coating of the active layer (thickness $\sim 90$ nm), annealing for 10 min at 100, 140 or at even higher temperatures (160–180 °C) was performed (in dark and in a nitrogen filled glove box), followed by evaporation of the metal electrodes. The current-voltage characteristics were measured with a Keithley 2400 Source Meter under AM 1.5G illumination with an intensity of 100 mW cm$^{-2}$ from a solar simulator (Model SS50A, Photo Emission Tech., Inc.).[25] Mild annealing of TQ1:$PC_{61}BM$ as well as TQ1:$PCBM_{8:2}$ at $100\,°C$ resulted in a comparable drop in $V_{oc}$ by $\sim 70$ mV (Fig. 4). However, for both sets of devices a slight improvement in $J_{sc}$ and $FF$ gave rise to an overall improvement in photovoltaic performance, which we have previously explained with local changes in the blend nanostructure that occur despite annealing below $T_g^{blend} \sim 110\,°C$. In contrast, annealing of the active layer at

140 or higher temperatures reduced the performance of corresponding devices. Whereas no significant change in $V_{oc}$ and $FF$ occurred, we observed large variations in $J_{sc}$. Annealing of TQ1:$PC_{61}BM$ films at $140\,°C$ resulted in a close to complete loss in $J_{sc}$ from an initial 7 mA cm$^{-2}$ to only 2 mA cm$^{-2}$. In strong contrast, TQ1:$PCBM_{8:2}$ active layers treated at the same conditions yielded devices that largely retained the initial photocurrent and still offered a $J_{sc} \sim 7$ mA cm$^{-2}$. Overall, annealing at $140\,°C$ effectively diminished the maximum power point (MPP) of reference TQ1:$PC_{61}BM$ but only resulted in a $\sim 20\%$ decrease in MPP for TQ1:$PCBM_{8:2}$. We rationalize this pronounced difference in device performance with the detrimental growth of micrometre-sized $PC_{61}BM$ crystals in case of TQ1:$PC_{61}BM$ but preservation of a more fine-grained TQ1:$PCBM_{8:2}$ nanostructure.

In conclusion, we have demonstrated that fullerene crystallization in mixtures of the two most commonly used fullerene derivatives, $PC_{61}BM$ and $PC_{71}BM$, is strongly suppressed at annealing temperatures that are suitable for roll-to-roll printing processes. Hence, the detrimental growth of micrometer-sized fullerene crystals is prevented in TQ1:PCBM films despite annealing above the glass transition temperature of the blend, which considerably enhances the thermal stability of the blend nanostructure. Clearly, the use of fullerene mixtures is a viable strategy to retain the photovoltaic performance of polymer solar cells blends, which would otherwise rapidly deteriorate at elevated temperatures. Moreover, the use of fullerene mixtures promises to reduce the cost of the acceptor material.

[1]Z. He, C. Zhong, S. Su, M. Xu, H. Wu, and Y. Cao, Nat. Photonics **6**, 591 (2012).

[2]S. H. Liao, H. J. Jhuo, Y. S. Cheng, and S. A. Chen, Adv. Mater. **25**, 4766 (2013).

[3]F. C. Krebs, Sol. Energy Mater. Sol. Cells **93**, 394–412 (2009).

[4]M. Jørgensen, K. Norrman, S. A. Gevorgyan, T. Tromholt, B. Andreasen, and F. C. Krebs, Adv. Mater. **24**, 580 (2012).

[5]S. Bertho, I. Haeldermans, A. Swinnen, W. Moons, T. Martens, L. Lutsen, D. Vanderzande, J. Manca, A. Senes, and A. Bonfiglio, Sol. Energy Mater. Sol. Cells **91**, 385 (2007).

[6]S. Bertho, G. Janssen, T. J. Cleij, B. Conings, W. Moons, A. Gadisa, J. D'Haen, E. Goovaerts, L. Lutsen, J. Manca, and D. Vanderzande, Sol. Energy Mater. Sol. Cells **92**, 753 (2008).

[7]C. Müller, J. Bergqvist, K. Vandewal, K. Tvingstedt, A. S. Anselmo, R. Magnusson, M. I. Alsonso, E. Moons, H. Arwin, M. Campoy-Quiles, and O. Inganäs, J. Mater. Chem. **21**, 10676 (2011).

[8]J. Bergqvist, C. Lindqvist, O. Bäcke, Z. Ma, Z. Tang, W. Tress, S. Gustafsson, E. Wang, E. Olsson, M. R. Andersson, O. Inganäs, and C. Müller, J. Mater. Chem. A **2**, 6146–6152 (2014).

[9]X. Yang, J. K. J. van Duren, R. A. J. Janssen, M. A. J. Michels, and J. Loos, Macromolecules **37**, 2151 (2004).

[10]C. Lindqvist, A. Sanz-Velasco, E. Wang, O. Bäcke, S. Gustafsson, E. Olsson, M. R. Andersson, and C. Müller, J. Mater. Chem. A **1**, 7174 (2013).

[11]B. Conings, S. Bertho, K. Vandewal, A. Senes, J. D'Haen, J. Manca, and R. A. J. Janssen, Appl. Phys. Lett. **96**, 163301 (2010).

[12]H. W. Liu, D. Y. Chang, W. Y. Chiu, S. P. Rwei, and L. Wang, J. Mater. Chem. **22**, 15586 (2012).

[13]C. Y. Chen, C. S. Tsao, Y. C. Huang, H. W. Liu, W. Y. Chiu, C. M. Chuang, U. S. Jeng, C. J. Su, W. R. Wu, W. F. Su, and L. Wang, Nanoscale **5**, 7629 (2013).

[14]Y. Santo, I. Jeon, K. S. Yeo, T. Nakagawa, and Y. Matsuo, Appl. Phys. Lett. **103**, 073306 (2013).

[15]J. J. Richards, A. H. Rice, R. D. Nelson, F. S. Kim, S. A. Jenekhe, C. K. Luscombe, and D. C. Pozzo, Adv. Funct. Mater. **23**, 514 (2013).

[16]C. Lindqvist, J. Bergqvist, C.-C. Feng, S. Gustafsson, O. Bäcke, N. D. Treat, C. Bounioux, P. Henriksson, R. Kroon, E. Wang, A. Sanz-Velasco, P. M. Kristiansen, N. Stingelin, E. Olsson, O. Inganäs, M. R. Andersson, and C. Müller, "Fullerene nucleating agents: A route towards thermally stable photovoltaic blends," Adv. Energy Mater. (published online).

[17]K. Tohji, A. Paul, L. Moro, R. Malhotra, D. C. Lorents, and R. S. Ruoff, J. Phys. Chem. **99**, 17785 (1995).

[18]L. V. Tsetkova, V. A. Keskinov, N. A. Charykov, N. I. Alekseev, E. G. Gruzinskaya, K. N. Semenov, V. N. Postnov, and O. A. Krokhina, Russ. J. Gen. Chem. **81**, 920 (2011).

[19]L. M. Andersson, Y. Hsu, K. Vandewal, A. B. Sieval, M. R. Andersson, and O. Inganäs, Org. Electron. **13**, 2856 (2012).

[20]D. F. Kronholm, J. C. Hummelen, A. B. Sieval, and P. Van't Hof, patent US 8,435,712 B2 (7 May 2013).

[21]R. Kroon, R. Gehlhaar, T. T. Steckler, P. Henriksson, C. Müller, J. Bergqvist, A. Hadipour, P. Heremans, and M. R. Andersson, Sol. Energy Mater. Sol. Cells **105**, 280 (2012).

[22]E. Wang, J. Bergqvist, K. Vandewal, Z. Ma, L. Hou, A. Lundin, S. Himmelberger, A. Salleo, C. Müller, O. Inganäs, F. Zhang, and M. R. Andersson, Adv. Energy Mater. **3**, 806 (2013).

[23]E. Wang, L. Hou, Z. Wang, S. Hellström, F. Zhang, O. Inganäs, and M. R. Andersson, Adv. Mater. **22**, 5240 (2010).

[24]Y. Kim, H. R. Yeom, J. Y. Kim, and C. Yang, Energy Environ. Sci. **6**, 1909 (2013).

[25]See supplementary material at http://dx.doi.org/10.1063/1.4870997 for UV-vis spectra and current-voltage device characteristics.

[26]C. Lindqvist, E. G. Wang, M. R. Andersson, and C. Müller, Macromol. Chem. Phys. **215**, 530–535 (2014).